Physicochem. Probl. Miner. Process., 57(4), 2021, 63-77

http://www.journalssystem.com/ppmp

Physicochemical Problems of Mineral Processing

ISSN 1643-1049

Received April 16, 2021; reviewed; accepted June 03, 2021

Evaluation of the efficiency of metal recovery from printed circuit boards using gravity processes

Dawid M. Franke [1], Tomasz Suponik [1], Paweł M. Nuckowski [2], Justyna Dubaj [3]

[1] Institute of Mining, Faculty of Mining, Safety Engineering and Industrial Automation, Silesian University of Technology, 2 Akademicka Street, 44-100 Gliwice, Poland; dawid.franke@polsl.pl; tomasz.suponik@polsl.pl;

[2] Materials Research Laboratory, Faculty of Mechanical Engineering, Silesian University of Technology, 18A Konarskiego Street, 44-100 Gliwice, Poland; pawel.nuckowski@polsl.pl

[3] Health and Safety Inspectorate, Silesian University of Technology, 2 Akademicka Street, 44-100 Gliwice, Poland; justyna.dubaj@polsl.pl

Corresponding author: dawid.franke@polsl.pl (Dawid Franke)

Abstract: This paper evaluates the efficiency of metal recovery from printed circuit boards (PCBs) using two gravity separation devices: a shaking table and a cyclofluid separator. The test results were compared with the results obtained from previous research, where an electrostatic separation process was used for an identically prepared feed. The feed for the separators consisted of PCBs shredded in a knife mill at cryogenic temperatures. The separation efficiency and purity of the products were evaluated based on microscopic analysis, ICP-AES, SEM-EDS, XRD, and specific density. The yield of concentrates (valuable metals) obtained from the shaking table and the cyclofluid separator amounted to 25.7% and 18.9%, respectively. However, the concentrate obtained from the cyclofluid separator was characterised by much higher purity, amounting to ~88% of valuable metals, compared to ~72% for the shaking table. In both cases, middlings formed a significant share, their yield amounting to ~25%, with the share of valuable metals of ~15%. The yield of waste obtained from the shaking table and the cyclofluid separator were 42.6% and 52.5%, respectively. In both cases, as a result of the applied process, the waste was divided into two homogeneous groups differing in grain size and shape. The recovery of metals through gravity separation is possible, in particular, by using a shaking table. These processes can also be applied to separate waste (plastics) into two groups to be selectively processed to produce new materials in line with a circular economy.

Keywords: metals recovery, printed circuit board, gravity separation, ICP-AES, SEM-EDS

1. Introduction

Electronic waste is an increasing challenge to the modern world driven by the doctrines of circular economy and sustainable development (Geissdoerfer et al., 2017; Kumar et al., 2015). As a result of technological progress, more and more waste of electrical and electronic equipment (WEEE) is produced, containing various hazardous additives and substances, such as mercury, brominated flame retardants, and chlorofluorocarbons or hydrochlorofluorocarbons (Forti et al., 2020). In addition, almost all WEEE contains printed circuit boards (PCBs) (Kumar et al., 2015), rich in valuable metals, the share of which is significantly higher than in natural metal ores (Dascalescu et al., 1992; Johnson et al., 2007). Therefore, despite the already known WEEE recycling technologies (Huang et al., 2009; Li et al., 2007; Schluep et al., 2006), it is necessary to carry on research to develop environmentally friendly and cost-effective technologies that can be applied in specific business and industrial conditions of a given country, using the existing technological installations and other technical resources.

PCBs are estimated to contain 30% of metals (hereinafter referred to as metals) in a free state and 70% of components such as glass fibre reinforced epoxy resin and polyesters (hereinafter referred to as

DOI: 10.37190/ppmp/138471

plastics) (Huang et al., 2009; Kumar et al., 2018a). PCBs are divided into different types depending on the purpose, but the most popular and most frequently used ones are FR-4 (Weil and Levchik, 2004). The plastic part of FR-4 mainly consists of SiO_2 (approx. 40%), CaO (approx. 20%), and, to a lesser extent, Al_2O_3, MgO, and BaO (Muniyandi, 2014). In addition, to improve the thermal resistance properties of PCBs, flame retardants (bromine and antimony compounds) are added (Duan et al., 2016). It is estimated that the metallic part of PCBs is composed of approx. 16% Cu, 3% Fe, 3% Sn, 2% Pb, 1% Zn, as well as Al, Ni, Cr, Na, Cd, Mo, Ti, and Co in smaller amounts (Bizzo et al., 2014; Kumar et al., 2018b). What is worth noting is the share of noble metals such as Au, Ag, and Pd, mainly used as contact metals (Cayumil et al., 2016), which is estimated to amount to 0.05%, 0.03%, and 0.01%, respectively (Charles et al., 2017).

Among the methods of recovering metals from PCBs, chemical and physical processes can be distinguished. The use of chemical methods often involves interference with the natural environment by discharging pollutants into the water and air (Leung et al., 2007; Qiu et al., 2020; Xiang et al., 2007) and generating waste. Currently, the most commonly used methods include pyrometallurgical, hydrometallurgical, biohydrometallurgical (Kaya, 2017), and plasma (Changming et al., 2018) separation. The last two can be classified as environmentally friendly. Still, in the case of biohydrometallurgy, the disadvantage is the long-term impact of micro-organisms on the components of PCBs during the catalysis of the metal recovery process. In the case of an installation for the production of metals via metallurgy functioning in a given region, it seems reasonable to separate metals from PCBs using cost-effective physical methods and process them in this installation. The non-metallic part (plastics) can then, following the principles of circular economy, be used to produce prefabricated elements, such as, for example, composite boards. The physical recovery methods include: electrostatic (Dascalescu et al., 1992; Franke et al., 2020; Jiang et al., 2009; Wu et al., 2008), magnetic (Suponik et al., 2019; Veit et al., 2005), and gravity separation in the air (Eswaraiah et al., 2008; Yoo et al., 2009) and water medium (Duan et al., 2009; Zhu et al., 2020). Metal recovery from PCBs can also be carried out by flotation using flotation reagents (Gallegos-Acevedo et al., 2014; Otunniyi et al., 2013) or without them (Ogunniyi and Vermaak, 2009). One of the popular gravity methods of metal recovery is separation on a shaking table, enabling the effective separation of metals from plastics (Burat and Özer, 2018; Zhu et al., 2020). In all these methods, it is necessary to adjust the degree of grinding and release the valuable substance, i.e., metals in the free state.

This research aimed to evaluate the efficiency of metal recovery from PCBs via two methods based on grain density difference: a shaking table and a cyclofluid separator, for the option, verified in the paper (Suponik et al., 2021), of grinding the feed (PCBs) in a knife mill with the use of liquid nitrogen as a medium for lowering the process temperature.

2. Materials and methods

2.1. Material

Popular motherboards from well-known manufacturers such as Intel, MSI, Asus, Nvidia, and Gigabyte were used in the study. The boards were disassembled from damaged or obsolete desktops assembled in 2007-09. The dismantled PCBs belonged to the most numerous group of FR-4, the laminate of which consists of glass fibre and epoxy resin (Sanapala, 2008). To minimise the diversity of material properties and thus facilitate the grinding process, the following elements have been removed from the boards: resistors, transistors, capacitors, EMI filters, connectors, batteries, chips, screws, and switches (Lee et al., 2012). Simple workshop tools were used for the disassembly process.

2.2. Grinding and preparation of feed for gravity separators

The feed for the LMN-100 knife mill by TestChem consisted of PCB parts cut into 3 cm x 3 cm pieces. The grinding was performed at cryogenic temperatures (<-150^{o}C). The cooling of the feed was carried out by placing the material in a container with liquid nitrogen. The cooling time was defined as the time from placing the material in the container until the liquid nitrogen ceased to boil and was equal to approximately 1 minute per 20 grams of material. The grinding parameters were as follows: sieve perforation in the mill 1 mm, mill load 20 g/min, rotator speed 2815 rpm, the gap between the knives

0.5 mm. The method of grinding with the use of various process parameters was the subject of the research presented in the paper (Suponik et al., 2021), where an electrostatic separator was used to separate metals from plastics after the grinding process. Due to the difficulties in dampening some parts of the ground material and the presence of grains with a density lower than that of water (Tuncuk et al., 2012), the feed for gravity separation was carried out in an aqueous medium was adequately prepared. For this purpose, before separation, the material was placed in a mechanical mixer for approx. 30 minutes, and then floating grains were collected from the water surface. These grains were not included in the gravity processes.

2.3. Gravity separation in an aqueous medium

Two devices for gravity separation of fine grains were used in the study: a shaking table (ST) and a cyclofluid separator (CS). The ST was equipped with a slatted aluminium plate, two independent nozzles for feeding water, and a feeder. As a result of separation, it is possible to obtain ten feed separation products. The separation of products into concentrate, middlings and waste resulted from the difference in the specific density of the grains. Based on previous observations (Franke et al., 2020; Suponik et al., 2021), the concentrate included products with a specific density >7.5 g/cm^3, the middlings included grains with a density of 7.4-3.5 g/cm^3, and waste I and II included grains with densities of 3.4-2.5 g/cm^3 and <2.4 g/cm^3, respectively. The separation parameters were as follows: table load: 9 dm^3/min (water with the material); the mass of material used for testing: 400 g, water flow rate of the first nozzle 5.7 dm^3/min, a water flow rate of the second nozzle 5.4 dm^3/min; table stroke 1.5 mm; table movement frequency 260 strokes/min; longitudinal slope angle: 1˚; transverse slope angle: 6˚; duration of separation: 3 min 45 sec.

The second method of separation was carried out in the CS (Fig. 1). For this purpose, a laboratory cyclofluid separator was built. Its operating principle corresponding to the operation of a semi-industrial U-shaped cyclofluid separator with continuous motion (patent application no. P.424161, Poland). The main elements of the laboratory CS structure were a cylindrical tank filled with water and a separation chamber immersed in it. The chamber was equipped with a sieve with a mesh size of 0.5 mm in the lower part. In the upper part, a drive was fixed that caused a vertical movement of its medium. The principle of operation is based on separation by cyclic fluidisation of the grains from the suspension according to their different densities. The pulsating and vertical movement of the liquid in the working chamber immersed in the tank exerts a thrust force on the grains. The stream lifts and loosens the material, and after it is throttled, the grains fall and are stratified by density. After the separation process is completed, the layers of products with specific densities are formed in the separation chamber – with grains characterised by the highest densities at the bottom of the cylinder. In the case of ground PCBs, no layers with visible characteristic boundaries were formed. Therefore, the contents of the chamber were separated into 0.5 cm-high layers. Layers of similar densities were combined: concentrate I consisted of products with a density above 8.5 g/cm^3; concentrate II consisted of material with a density from 8.4 to 8.0 g/cm^3; middlings I from 7.9 to 6.5 g/cm^3; middlings II from 6.4 to 5.0 g/cm^3; intermediate III from 4.9 to 3.5 g/cm^3; and waste I and II from 3.4 to 2.5 g/cm^3 and <2.4 g/cm^3, respectively. To increase the thrust force (liquid stream) acting on the grains, a band with one-way valves was attached to the body of the working chamber. The upward movement of the working chamber caused the valves to open, and when the direction of movement was changed, they were closed. The parameters of the separation process in the CS were as follows: volume of used water 13 dm^3, material density - 200 g of material per 0.5 dm3 of water; separation chamber stroke 4 cm; separation chamber movement frequency 53 movements/minute; duration of separation: 1 min. 30 sec.

2.4. Product analysis

The purity of the concentrates, middlings, and waste was evaluated using Inductively Coupled Plasma Atomic Emission Spectroscopy (ICP-AES), specific density analysis using a pycnometer and ethyl alcohol (PN-EN 1097-7: 2001), Scanning Electron Microscope (SEM) with Energy Dispersive X-ray Spectroscopy (EDS), and microscopic analysis using Stereo Microscope and X-ray Powder Diffraction (XRD). The following analyses were carried out for the separation products obtained from the shaking table and cyclofluid separator:

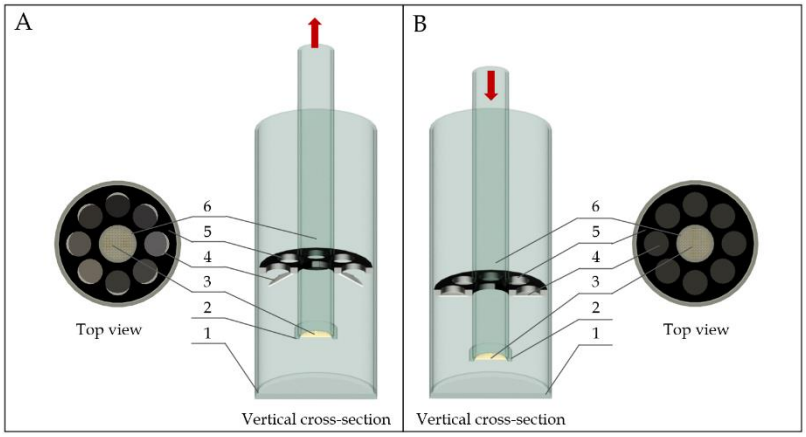

Fig. 1. Diagram of a laboratory cyclofluid separator: A – upper position, B – lower position, 1 – cylindrical tank ($Ø_{in}$ 19.5 cm), 2 – sieve clamp, 3 – sieve (mesh size 0.5 x 0.5 mm), 4 – valves, 5 – band, 6 – separation (working) chamber: $Ø_{in}$ 5 cm

- ICP-AES – using the Jy2000 spectrometer (by Yobin-Yvon) to assess the share of elements in products. The source of the induction was a plasma torch coupled with a 40.68 MHz frequency generator. The products were diluted beforehand;
- Specific density – with the use of Gay-Lussac pycnometers based on PN-EN 1097-7:2001 with the use of ethyl alcohol with a density of 0.7893 g/cm^3;
- Microscopic – using the Modular Stereo Microscope, Zeiss SteREO Discovery (Carl Zeiss AG, Germany).

The following additional analyses were carried out for the concentrates and middlings obtained as a result of separation:

- High resolution scanning electron microscope Zeiss SUPRA 35 (Carl Zeiss AG, Germany), equipped with EDAX Energy Dispersive X-ray Spectroscopy (EDS) chemical analysis system (EDAX, US);
- Qualitative phase analysis was performed with the use of a Panalytical X'Pert Pro MPD diffractometer (Panalytical, the Netherlands), utilising filtered radiation of a cobalt-anode lamp ($\lambda K\alpha$ = 0.179 nm). The diffraction lines were recorded in Bragg-Brentano geometry, using the step-scanning method by means of a PIXcell 3D detector on the diffracted beam axis, in the angle range from 20–100° [2θ] (step 0.05°, count time per step 200s). The obtained diffractograms were analysed with the use of Panalytical High Score Plus (v. 3.0e) software with the PAN-ICSD database.

3. Results and discussion

The feed for both separators was the material shredded in a knife mill with the cooling of the PCBs to cryogenic temperatures. Detailed results of the feed grinding study are presented in the publication (Suponik et al., 2021). The particle size distribution of the feed is shown in Table 1. Due to the nature of the material, the analysis was carried out using sieves and particle size analyser. More detailed information on this material is provided in the article (Suponik et al., 2021).

As a result of separation on the ST, in line with the assumed separation, four products T1 - T4 were obtained, while on CS seven products C1 - C7 were obtained. Product yields and their densities are presented in Table 2 and 3, respectively. In both cases, the floating material, which constituted approx. 3% of the feed was removed before separation. This material was named T0 and C0 according to the process used. Considering that the density of metals is much higher than that of plastics and fibreglass, it can be concluded that this material did not contain any metallic parts.

The highest yield of concentrate was obtained for the ST. It was quantitatively comparable to the yield obtained in the research with the use of electrostatic separation (Suponik et al., 2021). Due to the construction of the CS, two groups of concentrate were obtained from this device: C1 – grains that passed through the sieve and C2 – grains that remained directly at the up of the sieve. The yield of these

Table 1. Particle size distribution of the feed (Suponik et al., 2021)

Grain Class, mm	Yield of the feed, %	
	Analysis carried out with Fritsch screens	Analysis carried out with the particle size analyser
>2.0	0.0	0.0
2.0–1.4	0.0	0.0
1.4–1.0	0.4	0.0
1.0–0.71	3.6	1.6
0.71–0.50	13.0	10.4
0.50–0.36	19.5	22.1
0.36–0.25	17.0	14.2
0.25–0.18	10.6	6.5
0.18–0.13	10.8	5.3
0.13–0.09	8.5	4.3
<0.09	16.6	35.6

groups amounted to less than 19%. For both analysed devices, a significant share was exhibited by separation middlings (T2 and C3 - C5), whose total yields were comparable for both processes and amounted to more than 25%, while the share of the intermediate obtained from electrostatic separation in the paper (Suponik et al., 2021) was much lower and amounted to less than 3%. Based on the density analysis, products T3, C6 and T4, C7 were classified as waste with comparable yields and densities. In both cases of separation, the most numerous wastes were T4 (33.7%) and C7 (44%), made up of the smallest grains.

An essential parameter for the assessment of the purity of separation products was their density. As the density increased, the metal share increased as well, while the lower the density, the higher the share of plastics and fibreglass. The highest density was obtained for t he product C1 (8.9 g/cm^3), followed by C2 (8.1 g/cm^3), and T1 (8.0 g/cm^3). The relatively low density of the concentrate obtained from the ST may indicate its high contamination with plastics and fibreglass. Referring to the research results presented in the publication (Suponik et al., 2021, p. 21), the product density of C1 was comparable to that of the concentrate resulting from electrostatic separation. The density of the product T2 was 4.5 g/cm^3, while the densities of the products C3 – C5 ranged from 7.0 g/cm^3 to 4.1 g/cm^3. The high density of the C3 product indicates the penetration of a high metal share into it – there is no clear boundary between the densities corresponding to the concentrates and middlings. The reason for the significant differences in the density of the middlings obtained from CS and the high density of the C3 product is the separation of the resulting material column into layers. The thickness of the C3 layer was 0.5 cm, which is the assumed minimum division into layers. If a cyclofluid separator was used on a semi-technical scale and the process was automated, the problem of the high density of the middlings could be eliminated and part of the material from C3 would go to the concentrate with the assumed density >7.5 g/cm^3. Waste densities for both devices were <3.1 g/cm^3.

For economic and environmental reasons, the amount of water used should also be noted. Water was continuously supplied to the ST separation processes. The water circuit can be closed, but in this case, the station should be equipped with a filtering installation to remove fine particles from the water. In the case of the CS, on the other hand, water is consumed as a result of filling the tanks and during the collection of products remaining on the sieve. During the tests with the use of the ST, about 77 dm^3 of water was used, while in the case of the CS it was only 13 dm^3, which makes it more economical and environmentally friendly in terms of water consumption. In both cases, however, the products obtained have to be dried, which also requires the use of energy. This problem does not exist in the case of electrostatic separation, which is carried out dry (Suponik et al., 2021).

Photographs of the products (made with a Zeiss microscope) obtained from the ST and CS are presented in Figures 2 and 3, respectively. In both cases, a characteristic separation of metallic grains from composed of plastics or fibreglass grains can be noticed. In the concentrates (Fig. 2a, 3a, and b), mainly homogeneous metallic grains were present, along with a small number of grains with a mixed

Table 2. Yield and density of products obtained from the shaking table

Products	T0	T1	T2	T3	T4
Yield of product, %	2.8	25.7	28.9	8.9	33.7
Amount of water in the product, dm^3	0.5	0.5	12.0	12.5	51.5
Specific density, g/cm^3	1.9	8.0	4.5	2.9	2.4

T0 – floating grains removed before the separation process

Table 3. Yield and density of products obtained from the laboratory cyclofluid separator

Products	C0	C1	C2	C3	C4	C5	C6	C7
Yield of product, %	3.1	6.4	12.5	12.1	7.1	6.3	8.5	44.0
Distance of layer from the sieve, cm	-	-	0÷0.5	0.5÷1	1÷1.5	1.5÷2	2÷3.5	3.5÷9.5
Specific density, g/cm^3	2.0	8.9	8.1	7.0	5.3	4.1	3.1	2.3

C0 – floating grains removed before the separation process

C1 – grains that have passed through the sieve

chemical composition (conglomerates) of metals, plastics, and fibreglass. However, there were no homogeneous grains composed of plastics and fibreglass. Taking into account all the products obtained, the concentrates showed the greatest variation in terms of grain size and shape. There were mainly irregular, polyhedral, globular, and patch grains. Compared to other concentrates, product T1 (Fig. 2a) exhibited the largest differences in size, while the largest share was exhibited by conglomerates composed of metals, plastics, and fibreglass. The T1 product was dominated by globular grains (ranging from 200 μm to 600 μm) and patch grains (patch thickness >30 μm; width of the most numerous ones □ 600 μm). The least numerous polyhedral grains exhibited transverse dimensions of approx. 400 μm. The shape of the irregular grains demonstrates that they were mostly formed as a result of crushing patch grains. In product C1 (Fig. 3a), the grains were smaller. This is connected to the use of a sieve with a mesh size of 0.5 mm in the CS separation process. Compared to other concentrates, no mixed grains composed of metals, plastics, and fibreglass were established in visible light. Globular grains (ranging from 200 μm to 450 μm) and patch grains (patch thickness> 30 μm; the width of the most numerous ones ranged from 200 μm to 350 μm) were predominant. The dimensions of the polyhedral grains were approx. 400 μm. The C2 product (Fig. 3b) was composed mainly of grains with a globular shape ranging from 500 μm to 850 μm, irregular and polyhedral (transverse dimensions ranging from 400 μm to 600 μm). The share of patch grains was the smallest (patch thickness >30 μm; width in the range of 500 μm to 850 μm).

The middlings were composed of a patch, fibrous, and globular grains. Compared to all other products, the largest grains were observed here. In the case of the T2 product (Fig. 2B), patch grains (with a width ranging from 200 μm to 1100 μm) with a layered structure characteristic of PCBs predominated. The thickness and width of these grains were greater compared to the patch grains found in the concentrates. The T2 product contained grains with a mixed chemical composition (conglomerates) of metals, plastics, and fibreglass, as well as homogeneous grains composed of plastics and fibreglass, mainly fibrous (fibre length up to 1800 μm) and globular (ranging from 600 μm to 1000 μm). In the C3 – C5 products, a gradually decreasing proportion of patch-shaped homogeneous metallic grains can be noticed. The C3 product (Fig. 3c) was composed of homogeneous, metallic patch grains (similar in size to T1), a few metallic polyhedral grains and mixed patch grains. However, there were no homogeneous grains composed of plastics and fibreglass. Such grains appeared in the C4 product (Fig. 3d) and, to a greater extent, in C5 (Fig. 3e). Large patch grains, approx. 2000 μm wide, appeared in the C4 and C5 products. These grains were probably "pushed through" the sieve in the knife mill as a result of the big forces in the grinding chamber.

The products T3 (Fig. 2c) and C6 (Fig. 3f) consisted mainly of fibrous, patch, and globular grains. In the case of the T3 product, fibrous grains (up to 2000 μm long) and patch grains (up to 800 μm wide) were the most numerous. The coloured grains (green, blue, and red) were of a globular shape. No metal-containing grains were found here, unlike the C6 product, where such grains were scarce but present.

Fibrous grains also predominated in the C6 product, but with more varied transverse dimensions. These fibrous grains ranged from the thickness of a single fibre to even 200 μm. Similarly to the T3 product, there were coloured globular grains. The products, T4 (Fig. 2d) and C7 (Fig. 3g), were composed of fibrous grains and a small amount of small globular grains (<100 μm) - mainly plastics, and a small amount of metallic powder, smaller than 20 μm. The C7 product contained fibrous grains characterised by a more variable size than in the case of the T4 waste.

As it can be seen, the largest share of large grains (over 700 μm) was established in middlings, and these grains were mostly composed of metal, plastic, and ceramic conglomerates. This may indicate that the middlings contain large amounts of grains with insufficient level of metal release from the remaining PCB parts and imperfections of gravity processes compared to electrostatic methods. Figs. 2c and 2d show that no metal grains were identified in the waste obtained from the ST. However, they may be covered with plastic and ceramic grains, which is confirmed by the results presented in Table 4. Additionally, this waste has been divided into two groups due to grain size, which may be advantageous in the case of its use – e.g., for the production of prefabricated products. The waste obtained from the CS was characterised by a higher share of metallic impurities and lower grain size uniformity. Fewer metallic grains were present in the intermediate and the waste obtained from the ST than in the case of the CS. The reason for the penetration of these grains towards the waste in the CS could lie in too wide a division into layers which, due to the limited size of the separation chamber, could not be reduced.

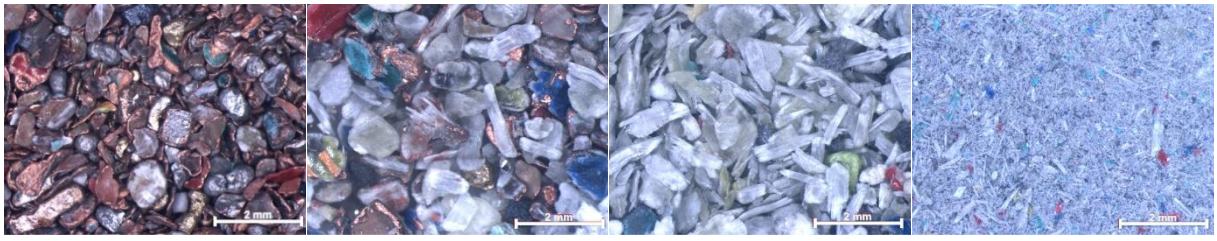

Fig. 2. Products obtained from the shaking table (stereo microscope): (a) – concentrate (T1), (b) – middling (T2), (c) – waste (T3), (d) – waste (T4)

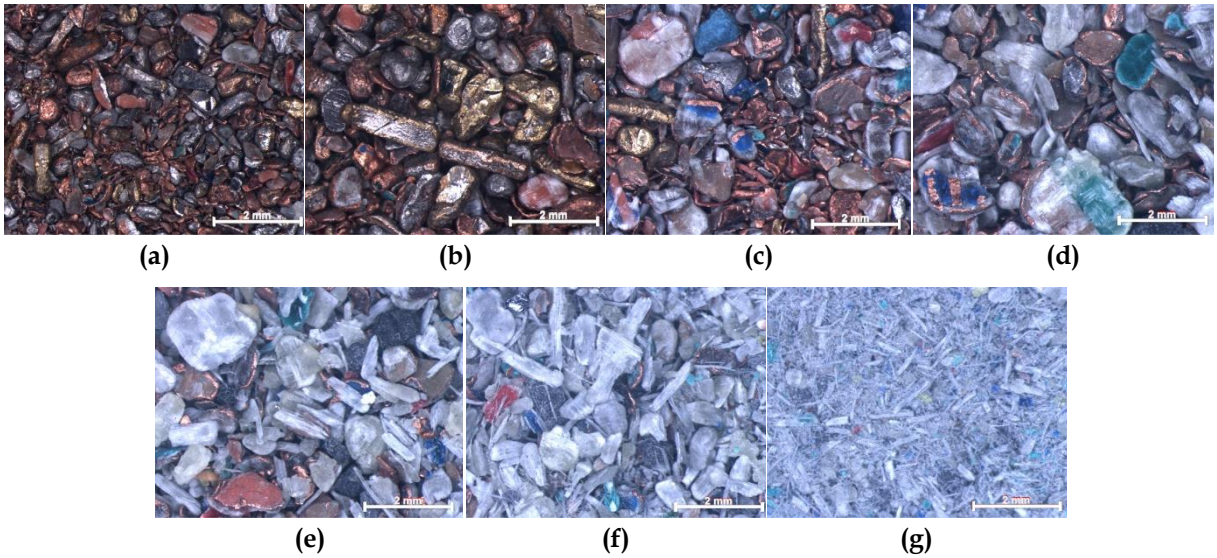

Fig. 3. Products obtained from the laboratory cyclofluid separator (stereo microscope): (a) – concentrate (C1), (b) – concentrate (C2), (c) – middling (C3), (d) – middling (C4), (e) – middling (C5), (f) – waste (C6), (g) – waste (C7)

The chemical composition of the feed and separation products was an important element in the evaluation of the efficiency of the separation processes used. The results of these studies are presented in Table 4. Based on the economic value, a separation into valuable and non-valuable elements was

introduced. Valuable elements include metals the recovery of which can lead to economic benefits and which are present in PCBs in free form. The second group of elements includes the components of epoxy resins, such as Sb, Ca, Br, Ba, Mg, Mn (Muniyandi, 2014), and Si as the main component of glass fibre (Kumar et al., 2018a). Unidentified components are probably components of epoxy resins (mainly polyphenols, less often polyglycols, and epichlorohydrin or oligomers) (Pham and Marks, 2005; Sood et al., 2010; Sood and Pecht, 2018). 17.70% Cu, 2.92% Sn, 0.0301 Ag, 0.0029 Au, 12.02% Sn, 6.56% Ca, 1.64% Br and other elements in low concentrations were identified in the feed (Table 4).

Attention should be paid to the tendencies of changes in the share of individual elements in the separation products. The proportion of valuable elements in the concentrates should be the highest, and non-valuable elements to be the lowest. Among the group of valuable elements, the share of almost all elements decreased towards waste. The exception was Al, the share of which was increasing. The largest share of this metal was identified in the T3 product, followed by T4, C5, and C6. Taking into account the density of this metal equal to 2.7 g/cm^3, in the case of using gravity separation, one could expect its values to vary in different separation products. The difference in the density of this metal is small to plastics and fibreglass, and the small Al grains may not have been fully separated and transferred to the group of grains with higher densities, i.e., to other metals. In the group of non-valuable elements, the shares of Ca, Br, and Si increased towards waste. The highest Sb share was identified in middlings, then in the concentrate, and the lowest in the waste.

In the products T1, C1, and C2, the following concentrations of all valuable metals were identified: 72.00%, 88.79%, and 88.78%, respectively. Among all concentrates, the T1 product contained the least valuable metals, i.e., 71.97%, including 59.20% Cu, 6.3% Sn, and 0.0098% Au. Similar shares were identified in C1 and C2: 88.79% in C1, including 72.10% Cu, 8.10% Sn% and 0.0096% Au, and 87.78% in C2, including 68.10% Cu, 11.40% Sn, and 0.0078% Au. The lowest share of the identified non-valuable elements in the concentrates, which translates into the highest purity of these products, characterised the C1 product, with this value equal to 7.13%, followed by the T1 product with 7.51%. The most contaminated concentrate was C2 with 12.55%. Similar shares of valuable and non-valuable elements were identified in the middlings, which amounted to ~16% and from ~16% to ~18%, respectively. The exception was the C5 product, which contained 6.81% of the identified valuable elements and 21.46% of non-valuable elements. The T3, T4, and C6 products, characterised as waste, contained a comparable amount of valuable and non-valuable elements, i.e. ~6% and ~22%, respectively. The C7 product was the least contaminated with metals, where the share of valuable elements was equal to 4.89%, with the share of non-valuable elements equal to 17.25%.

To examine the morphology of the concentrate and intermediate grains obtained from both gravity separation devices and to determine the chemical composition in the grain micro-areas, as well as to demonstrate the amount and type of metal, plastic, and ceramic or metal and metal conglomerates, photographs were taken (Fig. 4 and 5) via scanning electron microscope using the quadrant backscatter electron detection method (QBSD). Moreover, a local quantitative microanalysis of chemical composition (EDS) (Table 5 and 6) was carried out. These methods primarily allowed to identify the number and type of connections present in mixed grains. The differences in the contrast visible in the photographs (Figs. 4 and 5) may indicate a heterogeneous chemical composition of the grains. Elements with a higher atomic mass are characterised by light colour, in contrast with the elements with a lower atomic mass, which appear as dark areas in the figures. Very bright areas, which are formed as a result of the accumulation of surface charges by plastics, may be an exception.

In the T1 product (Fig. 4a), about half of the surface displayed in the picture is occupied by homogeneous grains (points 1^{T1}, 2^{T1}, 3^{T1}), composed mainly of Cu, Sn, Zn, and a small amount of Al (Table 5). These are mainly globular grains (with a diameter from ~100 μm to ~900 μm) and polyhedral grains (with a transverse dimension of ~350 μm). This product also contains fewer homogeneous patch grains with a diameter of less than 250 μm. Grains with a mixed chemical composition (metal, plastic, and ceramic conglomerates), manifested by high-contrast areas, are mainly patch and irregular grains of various sizes. As can be noticed, the patch grains are covered with a very thin layer of plastic and fibreglass. The T2 product (Fig. 4b) contains grains of mixed chemical composition and grains composed of plastics and fibreglass. Conglomerates constitute the vast majority of the intermediate and mainly take a patch (the diameter of the most numerous ones ranges from 400 μm to 700 μm) and irregular

shape. Compared to the T1 product (Fig. 4a), the proportion of grains <200 μm in diameter is much lower. The results of the chemical composition analysis for micro-areas 2^{T2} and 3^{T2} (Table 5) confirm the presence of Cu in mixed grains, which is still mechanically bonded to the PCB substrate composed of plastics and fibreglass. Due to their chemical composition, it can be assumed that these grains come from internal PCB layers. Grain with a diameter of ~2000 μm, marked with point 2^{T2} (Fig. 4b), was probably pushed through the knife mill sieve during grinding as a result of big forces occurring in the grinding chamber.

In the C1 product (Fig. 5a), homogeneous grains of globular (with the most numerous ones with a diameter of 200 μm to 450 μm), irregular and polyhedral shape (with a maximum transverse dimension up to 200 μm) constituted the largest share. The patch grains present there were small (the most numerous ones less than 100 μm in diameter). Differences in contrast in a small number of patch grains indicate a small number of conglomerates. The chemical composition of grains in the 1^{C1}-4^{C1} micro-areas (Table 6) indicates a high Cu share, which confirms the high purity of the concentrate. In the case of the C2 product (Fig. 5b), polyhedral grains (the most numerous ones with a transverse dimension of ~600 μm) had the largest share. Almost every analysed grain was composed of approximately 50% Cu, 11% Al, 11% Ni, 11% Zn, 9% Sn, 5% Si, 1.5% Ca, and 1% Fe (Table 6). The shape and chemical composition of the grains may indicate that they come from various contacts (sockets) present in the PCBs. Occasionally, irregular grains occurred (point 3^{C2}, Fig. 5b), the shape of which indicated deformed patch grains. Based on the differences in contrast visible in the photographs (Fig. 5b), it can be concluded that the grains are covered with a small layer of plastics and fibreglass. The C3 product is composed mainly of heterogeneous irregular and patch grains (the most numerous ones with a width ranging from 450 μm to 750 μm). Homogeneous metallic patch grains (up to 300 μm wide) were present to a small extent. The results of the chemical composition analysis showed that most of the grains present in the C3 intermediate were composed of Cu, Al, Sn, and Si. Small amounts of Ag were established in the micro-area 2^{C3}. No homogeneous grains composed of plastics and fibreglass have been identified here. The C4 product (Fig. 5d) also includes mainly heterogeneous, irregular grains and patch grains (the most numerous ones with a diameter ranging from 500 μm to 850 μm) and homogeneous fibrous grains (with a transverse dimension up to 300 μm). The results of the analysis of the chemical composition of fibrous grains (point 4^{C4}, Table 6) indicated that these grains were mainly composed of Si, which is the main component of the glass fibre.

For concentrates obtained from the shaking table and cyclofluid separator, an X-ray qualitative phase composition analysis was performed (Fig. 6). Low amounts of metallic or non-metallic phases may have

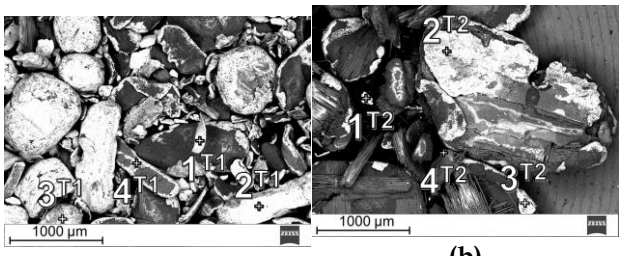

Fig. 4. The T1 and T2 products obtained from the shaking table (SEM, QBSD mode (Table 4) with marked EDS analysis points): (a) – product T1, (b) – product T2

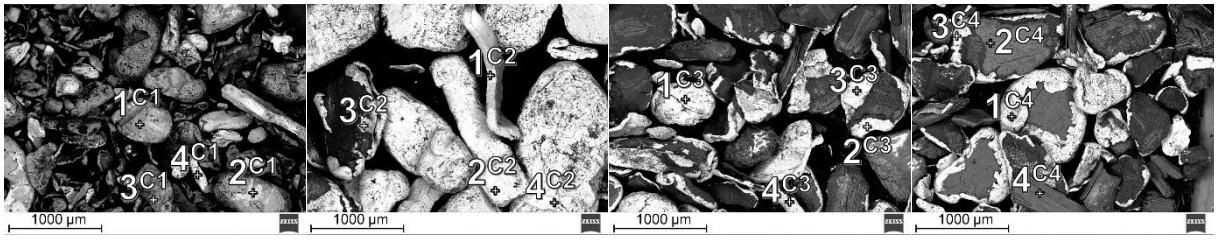

Fig. 5. Products obtained from the laboratory cyclofluid separator (s SEM, QBSD mode (Table 5) with marked EDS analysis points): (a) – product C1, (b) – product C2, (c) – product C3, (d) – product C4

Table 4. Elemental share in the feed and separation products [in %]

	Element	Feed	T1	T2	T3	T4	C1	C2	C3	C4	C5	C6	C7
Valuable elements	Cu	17.70	59.20	9.50	2.44	1.55	72.10	68.10	11.30	10.20	2.88	2.55	1.88
	Al	1.95	0.89	1.61	3.30	3.02	1.09	0.85	1.57	2.17	2.88	2.86	2.49
	Pb	0.39	1.10	0.64	0.02	0.02	1.50	1.40	0.88	0.91	0.05	0.02	0.01
	Zn	0.69	1.90	0.60	0.11	0.06	2.30	2.40	0.65	0.54	0.18	0.11	0.05
	Ni	0.19	0.59	0.19	0.08	0.06	1.09	1.07	0.32	0.36	0.08	0.06	0.01
	Fe	0.38	0.94	0.25	0.38	0.28	1.35	1.44	0.36	0.27	0.41	0.38	0.18
	Sn	2.92	6.30	2.67	0.27	0.36	8.10	11.40	1.10	0.90	0.10	0.11	0.07
	Cr	0.06	0.14	0.07	0.08	0.06	0.21	0.14	0.07	0.08	0.09	0.13	0.08
	Ti	0.26	0.91	0.15	0.13	0.09	0.99	0.89	0.24	0.21	0.15	0.21	0.13
	Ag	0.0301	0.0216	BDL	BDL	BDL	0.0582	0.0078	0.0012	BDL	BDL	BDL	BDL
	Au	0.0029	0.0072	BDL	BDL	BDL	0.0096	0.0078	BDL	BDL	BDL	BDL	BDL
	Sum	24.57	72.00	15.68	6.81	5.50	88.80	87.71	16.49	15.64	6.82	6.43	4.90
Non-valuable elements	Sb	0.22	0.10	0.34	0.18	0.11	0.50	0.30	0.09	0.08	0.15	0.17	0.12
	Ca	6.56	0.90	5.10	6.99	8.10	0.98	1.20	6.10	5.40	7.10	7.40	6.90
	Br	1.64	0.53	0.78	0.92	1.89	0.32	0.45	0.52	0.96	1.50	2.11	2.30
	Ba	0.31	0.71	0.15	0.19	0.12	0.92	0.84	0.09	0.07	0.21	0.25	0.22
	Si	12	3.10	9.30	15.10	13.10	0.92	5.50	6.30	9.20	13.80	15.20	9.80
	Mn	0.01	0.0065	0.0022	BDL	BDL	0.0078	0.0067	0.0054	0.0056	0.0077	0.0062	0.0012
	Sum	20.74	5.35	15.67	23.38	23.32	3.65	8.30	13.11	15.72	22.77	25.14	19.34

*BDL - below detection limit

DOI: 10.37190/ppmp/138471

Table 5. Element concentration [% at.] (EDS) in the micro-areas marked in Figure 4

Product	Point of analysis	Element concentration, % at.														
		Mg	Al	Al	Si	S	Ca	Ti	Cr	Fe	Ni	Cu	Zn	Ag	Sn	Ba
T1	1	-	-	-	-	-	-	-	-	2.7	-	92.2	-	-	5.1	-
	2	-	1	-	-	-	-	-	-	-	9	59.3	28.7	-	2	-
	3	-	1.2	-	1.4	-	-	-	-	-	51.4	34.8	11.2	-	-	-
	4	-	2.5	-	1.9	-	-	-	-	-	-	92.1	-	-	-	3.5
T2	1	-	2	-	3.6	-	-	44.8	-	-	-	-	7.2	-	-	42.4
	2	-	2.5	-	-	-	-	-	-	-	-	85.1	-	-	12.4	-
	3	-	11.3	-	14.5	-	-	-	-	-	-	74.2	-	-	-	-
	4	-	61.9	-	28.6	-	8.3	-	-	-	-	-	-	-	-	1.2

Table 6. Element concentration, [% at.] (EDS) in the micro-areas marked in Figure 5

Product	Point of analysis	Element concentration, % at.														
		Mg	Al	Al	Si	S	Ca	Ti	Cr	Fe	Ni	Cu	Zn	Ag	Sn	Ba
C1	1	-	-	-	-	-	-	-	-	0.6	-	99.4	-	-	-	-
	2	-	-	-	-	-	-	-	-	0.1	-	99.9	-	-	-	-
	3	-	-	8.4	-	-	-	-	-	-	-	91.6	-	-	-	-
	4	-	-	1.4	-	-	-	-	-	-	-	98.6	-	-	-	-
C2	1	-	10.8	-	4.7	-	1.6	-	-	1.9	11	50	11.3	-	8.7	-
	2	-	10.5	-	4.8	-	1.8	-	-	1.8	11.5	49.1	12.2	-	8.3	-
	3	-	10.7	-	4.7	-	1.7	-	-	1.7	12.9	48.3	11.8	-	9.2	-
	4	-	10.1	-	4.9	-	1.7	-	-	1.7	11.1	49.1	12.3	-	9.1	-
C3	1	1.3	18.9	-	18.3	-	-	-	-	-	-	9.3	-	-	52.2	-
	2	0.5	1.0	-	13.5	-	-	-	1.3	6.6	-	33.3	-	1.3	42.5	-
	3	-	4.1	-	-	-	-	-	-	-	2.5	56.2	-	-	37.2	-
	4	-	17.9	-	-	-	-	-	-	-	-	82.1	-	-	-	-
C4	1	-	10.2	-	4	-	1.5	-	1.5	5	-	74.3	3.5	-	-	-
	2	7.4	6.2	-	14.8	39.5	-	-	-	-	-	-	-	-	-	32.1
	3	-	-	-	-	-	-	-	-	4.7	-	95.3	-	-	-	-
	4	-	-	96.3	3.7	-	-	-	-	-	-	-	-	-	-	-

not been identified due to the limited sensitivity of the method. In each of the concentrates, diffraction lines were identified corresponding to Cu, tin bronze CuSn (3.68/0.32), Ni, and Sn phases. Conversely, no diffraction lines were established for the group of non-valuable elements, which may indicate a relatively high purity of the concentrates for a specific concentration range resulting from the detection of the measuring device.

Based on the conducted research, it can be concluded that the correlations between the density, yields, and the share of valuable and non-valuable elements may constitute a parameter determining the quality of separation products (Fig. 7). In the most optimal separation process, the concentrate should contain as many valuable elements as possible and thus should be characterised by the highest possible density. It should be the opposite in the case of waste, which should contain the least valuable elements and exhibit the lowest possible density. Comparing the quality of the products obtained from the shaking table, cyclofluid separator, and electrostatic separator (Fig. 7), it can be concluded that the best efficiency for the analysed material is provided by the electrostatic separator. It should be added that for this device, the amount of the middling is minimised and does not exceed 3%. In comparison with the other tested devices, i.e., the ST and CS, it is a value lower by more than 26% and 22%, respectively. However, it should be noted that the critical factor determining the efficiency of electrostatic separation is the size of the feed grains (Lu et al., 2008; Wu et al., 2009), unlike gravity separators, where the tolerance to grain size changes is greater. The recovery rates of valuable elements for the ST, CS and electrostatic separator were roughly 75%, 70%, 95%, respectively, while metal losses

DOI: 10.37190/ppmp/138471

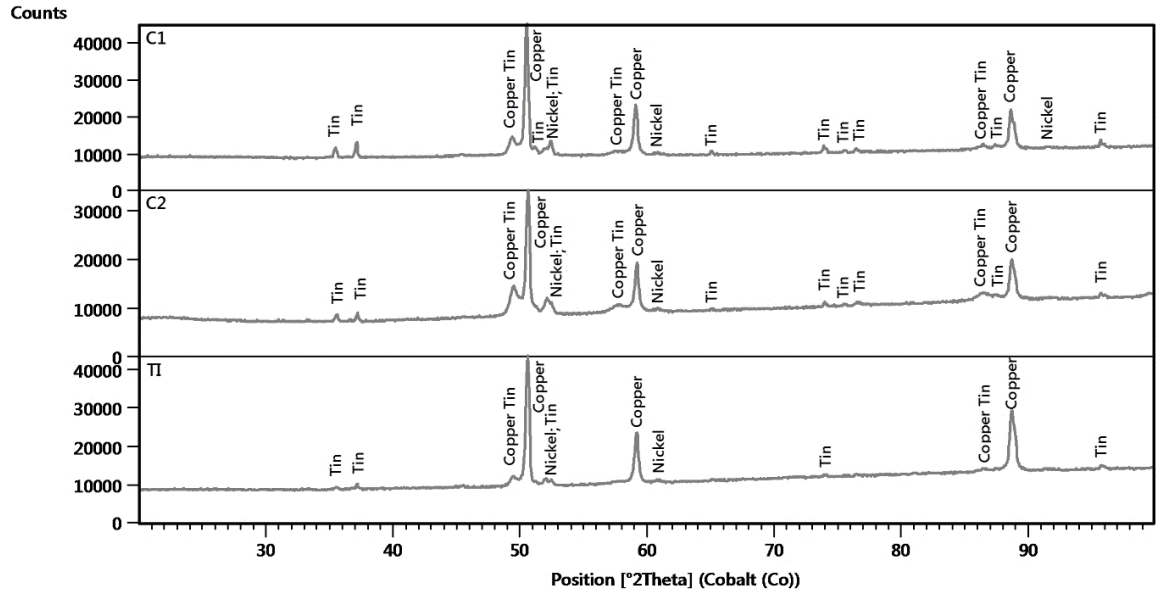

Fig. 6. X-ray diffraction patterns of C1, C2, and T1 products

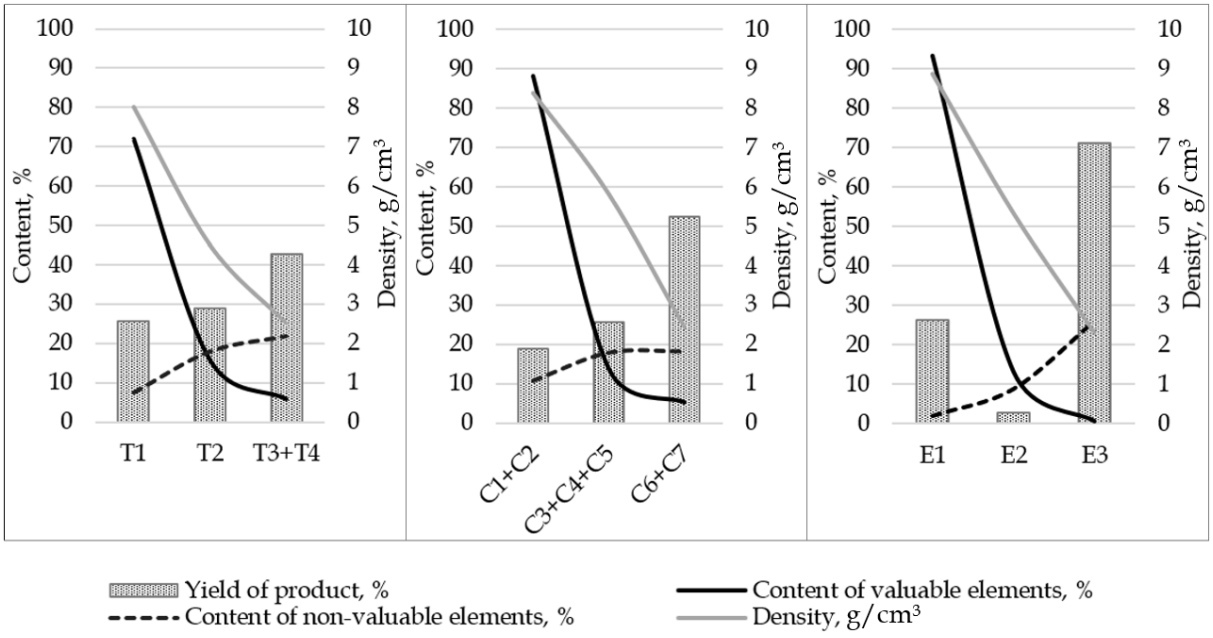

Fig. 7. Yield of separation products as a function of their density and quality parameters (valuable and non-valuable elements); E1 – concentrate, E2 – middlings, and E3 – waste from electrostatic separation (Suponik et al., 2021)

were 10%, 15% and 1%. In the case of the ST and CS, the content of valuable elements in the middlings was very high and amounted roughly 15%, in contrast to the electrostatic separator, in which it was 4%. As already mentioned, the middlings can be further processed, e.g. biohydrometallurgy or next grinding and processing.

4. Conclusions

The efficiency of metal recovery from ground PCBs using a shaking table and a cyclofluid separator is high. The yield of concentrate, intermediate, and waste obtained from the shaking table were 25.7%, 28.9, and 45.4%, respectively. For the cyclofluid separator these values were 18.9%, 31.7%, and 61.9%, respectively. In both cases, the obtained concentrates were characterised by relatively high purity, i.e., the content of valuable elements and the lack of contaminants, i.e., plastics and fibreglass. The

disadvantage of these processes was the high yield of middlings and the related losses of valuable elements.

Therefore, considering the environmental aspects (water consumption and energy consumption when drying the separation products) and the purity of all obtained products, the electrostatic separation presented in the paper (Suponik et al., 2021) seems to be a more favourable process for separating metals from plastics. Furthermore, gravity processes could be used as auxiliary operations, for example, to separate waste (i.e., the mixture of plastics obtained from electrostatic separation) into two groups according to grain size and shape to obtain substrates for the production of various composite materials. These processes could also prove to be highly effective in recovering metals from PCBs in the large variability of the grain composition of the feed.

Acknowledgments

Publication supported by Own Scholarship Fund of the Silesian University of Technology in the year 2019/2020, grant number: 26/FSW18/0003-03/2019.

References

BIZZO, W., FIGUEIREDO, R., DE ANDRADE, V., 2014. *Characterisation of Printed Circuit Boards for Metal and Energy Recovery after Milling and Mechanical Separation*. Materials 7, 4555–4566.

BURAT, F., ÖZER, M., 2018. *Physical separation route for printed circuit boards*. Physicochem. Probl. Miner. Process., 54(2), 554-566.

CAYUMIL, R., KHANNA, R., RAJARAO, R., MUKHERJEE, P.S., SAHAJWALLA, V., 2016. *Concentration of precious metals during their recovery from electronic waste*. Waste Manage. 57, 121–130.

CHANGMING, D., CHAO, S., GONG, X., TING, W., XIANGE, W., 2018. *Plasma methods for metals recovery from metal–containing waste*. Waste Manage. 77, 373–387.

CHARLES, R.G., DOUGLAS, P., HALLIN, I.L., MATTHEWS, I., LIVERSAGE, G., 2017. *An investigation of trends in precious metal and copper content of RAM modules in WEEE: Implications for long term recycling potential.* Waste Manage. 60, 505–520.

DASCALESCU, L., IUGA, A., MORAR, R., 1992. *Corona–Electrostatic Separation: An Efficient Technique for the Recovery of Metals and Plastics From Industrial Wastes*. Magn. Electr. Separ. 4, 241-255.

DUAN, C., WEN, X., SHI, C., ZHAO, Y., WEN, B., HE, Y., 2009. *Recovery of metals from waste printed circuit boards by a mechanical method using a water medium*. J. Hazard. Mater. 166, 478–482.

DUAN, H., HU, J., YUAN, W., WANG, Y., YU, D., SONG, Q., LI, J., 2016. *Characterising the environmental implications of the recycling of non-metallic fractions from waste printed circuit boards*. J. Clean. Prod.137, 546–554.

ESWARAIAH, C., KAVITHA, T., VIDYASAGAR, S., NARAYANAN, S.S., 2008. *Classification of metals and plastics from printed circuit boards (PCB) using air classifier*. Chem. Eng. Process. 47, 565–576.

FORTI, V., BALDÉ, C.P., KUEHR, R., BEL, G., 2020. *The Global E-waste Monitor 2020: Quantities, flows and the circular economy potential*. United Nations University (UNU)/United Nations Institute for Training and Research (UNITAR) – co-hosted SCYCLE Programme, International Telecommunication Union (ITU) & International Solid Waste Association (ISWA), 1-120.

FRANKE, D., SUPONIK, T., NUCKOWSKI, P.M., GOŁOMBEK, K., HYRA, K., 2020. *Recovery of Metals from Printed Circuit Boards By Means of Electrostatic Separation*. Management Systems in Production Engineering 28, 213–219.

GALLEGOS-ACEVEDO, P.M., ESPINOZA-CUADRA, J., OLIVERA-PONCE, J.M., 2014. *Conventional flotation techniques to separate metallic and non-metallic fractions from waste printed circuit boards with particles nonconventional size*. J. Min. Sci. 50, 974–981.

GEISSDOERFER, M., SAVAGET, P., BOCKEN, N.M.P., HULTINK, E.J., 2017. *The Circular Economy – A new sustainability paradigm?* J. Clean. Prod.143, 757–768.

HUANG, K., GUO, J., XU, Z., 2009. *Recycling of waste printed circuit boards: A review of current technologies and treatment status in China*. J. Hazard. Mater. 164, 399–408.

JIANG, W., JIA, L., ZHEN-MING, X., 2009. A new two-roll electrostatic separator for recycling of metals and nonmetals from waste printed circuit board. J. Hazard. Mater. 161, 257–262.

JOHNSON, J., HARPER, E.M., LIFSET, R., GRAEDEL, T.E., 2007. Dining at the Periodic Table: Metals Concentrations as They Relate to Recycling. Environ. Sci. Technol. 41, 1759–1765.

KAYA, M., 2017. *Recovery of Metals and Nonmetals from Waste Printed Circuit Boards (PCBs) by Physical Recycling Techniques*, in: ZHANG, L. et al. (Eds.), Energy Technology 2017. The Minerals, Metals & Materials Series. Springer, Cham., https://doi.org/10.1007/978-3-319-52192-3_43.

KUMAR, A., HOLUSZKO, M.E., JANKE, T., 2018A. *Characterisation of the non-metal fraction of the processed waste printed circuit boards*. Waste Manage. 75, 94–102.

KUMAR, A., KUPPUSAMY, V., HOLUSZKO, M., JANKE, T., 2018b. *Improving the Energy Concentration in Waste Printed Circuit Boards Using Gravity Separation*. Recycling 3, 21.

KUMAR, V., LEE, J., JEONG, J., JHA, M.K., KIM, B., SINGH, R., 2015. *Recycling of printed circuit boards (PCBs) to generate enriched rare metal concentrate*. J. Ind. Eng. Chem. 21, 805–813.

LEE, JAERYEONG, KIM, Y., LEE, JAE-CHUN, 2012. *Disassembly and physical separation of electric/electronic components layered in printed circuit boards (PCB)*. J. Hazard. Mater. 241–242, 387–394.

LEUNG, A.O.W., LUKSEMBURG, W.J., WONG, A.S., WONG, M.H., 2007. *Spatial distribution of polybrominated diphenyl ethers and polychlorinated dibenzo-p-dioxins and dibenzofurans in soil and combusted residue at Guiyu, an electronic waste recycling site in southeast China*. Environ. Sci. Technol. 15;41(8):2730-7

LI, J., LU, H., GUO, J., XU, Z., ZHOU, Y., 2007. *Recycle Technology for Recovering Resources and Products from Waste Printed Circuit Boards*. Environ. Sci. Technol. 41, 1995–2000.

LU, H., LI, J., GUO, J., XU, Z., 2008. *Movement behavior in electrostatic separation: Recycling of metal materials from waste printed circuit board*. J. Mater. Process. Technol. 197, 101–108.

MUNIYANDI, S.K., SOHAILI, J., HASSAN, A., 2014. Encapsulation of non-metallic fractions recovered from printed circuit boards waste with thermoplastic. J. Air. Waste. Manag .Assoc. 64:9, 1085-1092.

OGUNNIYI, I.O., VERMAAK, M.K.G., 2009. *Investigation of froth flotation for beneficiation of printed circuit board comminution fines*. Minerals Engineering 22, 378–385.

OTUNNIYI, I.O., VERMAAK, M.K.G., GROOT, D.R., 2013. *Particle size distribution and water recovery under the natural hydrophobic response flotation of printed circuit board comminution fines*. Mining, Metallurgy & Exploration 30, 85–90.

PHAM, H.Q., MARKS, M.J., 2005. *Epoxy Resins*. In Ullmann's Encyclopedia of Industrial Chemistry, (Ed.), Germany.

QIU, RUIJUN, LIN, M., RUAN, J., FU, Y., HU, J., DENG, M., TANG, Y., QIU, RONGLIANG, 2020. *Recovering full metallic resources from waste printed circuit boards: A refined review*. J. Clean. Prod.244, 118690.

SANAPALA, R., 2008. *Characterisation of FR-4 Printed Circuit Board Laminates Before and After Exposure to Lead-free Soldering Conditions*. M.S. thesis, Dept. Mech. Eng., Univ. Maryland, College Park, MD, USA.

SCHLUEP, M., HAGELUEKEN, C., KUEHR, R., MAGALINI, F., MAURER, C., 2009. *Recycling – from e-waste to resources*. Sustainable Innovation and Technology Transfer Industrial Sector Studies, Berlin, Germany.

SOOD, B., PECHT, M., 2018. *The effect of epoxy/glass interfaces on CAF failures in printed circuit boards*. Microelectronics Reliability 82, 235–243.

SOOD, B., SANAPALA, R., DAS, D., PECHT, M., HUANG, C.Y., TSAI, M.Y., 2010. *Comparison of Printed Circuit Board Property Variations in Response to Simulated Lead-Free Soldering*. IEEE Trans. Electron. Packag. Manufact. 33, 98–111.

SUPONIK, T., FRANKE, D., NUCKOWSKI, P., 2019. *Electrostatic and magnetic separations for the recovery of metals from electronic waste*. IOP Conf. Ser.: Mater. Sci. Eng. 641, 012017.

SUPONIK, T., FRANKE, D.M., NUCKOWSKI, P.M., MATUSIAK, P., KOWOL, D., TORA, B., 2021. *Impact of Grinding of Printed Circuit Boards on the Efficiency of Metal Recovery by Means of Electrostatic Separation*. Minerals 11, 281.

TUNCUK, A., STAZI, V., AKCIL, A., YAZICI, E.Y., DEVECI, H., 2012. *Aqueous metal recovery techniques from e-scrap: Hydrometallurgy in recycling*. Minerals Engineering 25, 28–37.

VEIT, H.M., DIEHL, T.R., SALAMI, A.P., RODRIGUES, J.S., BERNARDES, A.M., TENÓRIO, J.A.S., 2005. *Utilisation of magnetic and electrostatic separation in the recycling of printed circuit boards scrap*. Waste Manage. 25, 67–74.

WEIL, E.D., LEVCHIK, S., 2004. *A Review of Current Flame Retardant Systems for Epoxy Resins*. J. Fire Sci. 22, 25–40.

WU, J., LI, J., XU, Z., 2008. *Electrostatic separation for multi-size granule of crushed printed circuit board waste using two-roll separato*r. J. Hazard. Mater. 159, 230–234.

WU, J., QIN, Y., ZHOU, Q., XU, Z., 2009. *Impact of nonconductive powder on electrostatic separation for recycling crushed waste printed circuit board*. J. Hazard. Mater. 164, 1352–1358.

XIANG, D., MOU, P., WANG, J., DUAN, G., ZHANG, H.C., 2007. *Printed circuit board recycling process and its environmental impact assessment*. Int. J. Adv. Manuf. Technol. 34, 1030–1036.

YOO, J.-M., JEONG, J., YOO, K., LEE, J., KIM, W., 2009. *Enrichment of the metallic components from waste printed circuit boards by a mechanical separation process using a stamp mill*. Waste Manage. 29, 1132–1137.

ZHU, X., NIE, C., WANG, S., XIE, Y., ZHANG, H., LYU, X., QIU, J., LI, L., 2020. *Cleaner approach to the recycling of metals in waste printed circuit boards by magnetic and gravity separation*. J. Clean. Prod.248, 119235.